The ''Electrostatic-Switch'' Mechanism: Monte Carlo Study of MARCKS-Membrane Interaction

Shelly Tzlil,* Diana Murray,† and Avinoam Ben-Shaul*
*Department of Physical Chemistry and The Fritz Haber Research Center, Hebrew University of Jerusalem, Jerusalem 91904, Israel; and †Department of Pharmacology, Columbia University, New York, New York 10032

ABSTRACT The binding of the myristoylated alanine-rich C kinase substrate (MARCKS) to mixed, fluid, phospholipid membranes is modeled with a recently developed Monte Carlo simulation scheme. The central domain of MARCKS is both basic ($\zeta = +13$) and hydrophobic (five Phe residues), and is flanked with two long chains, one ending with the myristoylated N-terminus. This natively unfolded protein is modeled as a flexible chain of ''beads'' representing the amino acid residues. The membranes contain neutral ($\zeta = 0$), monovalent ($\zeta = -1$), and tetravalent ($\zeta = -4$) lipids, all of which are laterally mobile. MARCKS-membrane interaction is modeled by Debye-Hückel electrostatic potentials and semiempirical hydrophobic energies. In agreement with experiment, we find that membrane binding is mediated by electrostatic attraction of the basic domain to acidic lipids and membrane penetration of its hydrophobic moieties. The binding is opposed by configurational entropy losses and electrostatic membrane repulsion of the two long chains, and by lipid demixing upon adsorption. The simulations provide a physical model for how membrane-adsorbed MARCKS attracts several PIP_2 lipids ($\zeta = -4$) to its vicinity, and how phosphorylation of the central domain ($\zeta = +13$ to $\zeta = +7$) triggers an ''electrostatic switch'', which weakens both the membrane interaction and PIP_2 sequestration. This scheme captures the essence of ''discreteness of charge'' at membrane surfaces and can examine the formation of membrane-mediated multicomponent macromolecular complexes that function in many cellular processes.

INTRODUCTION

A delicate balance between the energetic and entropic contributions to the membrane adsorption free energy is exhibited in various biological processes (1,2). One important example is the ''electrostatic switch'' mechanism underlying the membrane binding of several proteins, including the myristoylated alanine-rich C kinase substrate (MARCKS) (3,4). This natively unfolded protein is thought to bind electrostatically to anionic lipids in the inner leaflet of the plasma membrane through its relatively small (25 residues) but strongly charged effector domain (ED), which comprises 13 basic residues (5–7). The effector domain also contains five phenylalanine residues. One end of the ED is connected to a flexible, 151-residue long, polypeptide chain, hereafter the ''loop'', ending at the myristoylated N-terminus. A comparably long flexible chain, hereafter the ''tail'', originates at the other end of the ED, ending at the C-terminus (Fig. 1).

Electrostatic attraction between the basic residues along the ED and the acidic membrane lipids, such as the multivalent phosphatidylinositol 4,5 bisphosphate (PIP_2) and the monovalent phosphatidylserine (PS) molecules, provides the major driving force for membrane adsorption of MARCKS. In addition, MARCKS-membrane binding is enhanced by the hydrophobic insertion of the five phenylated ED residues, as well as of the myristoylated N-terminus anchor. On the other hand, and apart from the loss of translational entropy attendant upon any adsorption process, two entropy loss mechanisms can detract from the free energy of membrane binding: i), The lower conformational freedom of the adsorbed protein because of excluded volume repulsive interactions with the membrane surface. This entropy loss involves mainly the long tail and loop chains, but also, though to a lesser extent, the ED. ii), The reduced ''mixing entropy'' of the lipid membrane resulting from the protein-induced sequestration of charged lipids, primarily PIP_2, and their localization to the vicinity of the basic protein domain. MARCKS adsorption is also expected to be opposed by electrostatic repulsion of the moderately negatively charged tail and loop from the acidic membrane. Similarly subtle interplays between energetic and entropic contributions to protein-membrane binding are likely to be encountered in a variety of signaling events (5,8).

Experiments suggest that the basic protein domain binds preferentially to the multivalent lipid PIP_2, ~3 PIP_2 molecules per adsorbed protein (9–11). The PIP_2 charge (which generally varies between −3 and −5 (12),) is assumed to have a valence of $\zeta = -4$ in this and previous studies, implying that a few multivalent lipids are sufficient to provide full electrostatic neutralization of the 13 ED charges (5,12). This is especially significant considering that the PIP_2 concentration in the plasma membrane is just ~1%, whereas the concentration of monovalent acidic lipids (primarily PS) is typically 10–30%. PIP_2, an important signaling lipid, acts at several levels to regulate cell structure and metabolism (13). For example, phospholipase C (PLC) hydrolyzes PIP_2 lipids in response to hormonal signals, yielding two fragments that serve as intracellular second messengers (8). PIP_2 may also interact with actin-binding proteins, thereby regulating cytoskeleton-membrane attachment (14). It is thus believed that

Submitted February 29, 2008, and accepted for publication April 25, 2008.
Address reprint requests to Avinoam Ben-Shaul, E-mail: abs@fh.huji.ac.il.
Editor: Helmut Grubmüller.

0006-3495/08/08/1745/13 $2.00
doi: 10.1529/biophysj.108.132522

by binding to PIP_2 lipids, MARCKS controls their accessibility for interaction with other cellular proteins (15–17). Indeed, phosphorylation of three serine residues in the MARCKS-ED by protein kinase C (PKC) reduces its net charge from +13 to +7. The decrease in electrostatic attraction between MARCKS and membrane is thought to contribute to the dissociation of MARCKS from the plasma membrane, exposing the PIP_2 lipids to hydrolysis by PLC and other reactions. This reversible binding of MARCKS to the lipid membrane underlies the ''electrostatic-switch mechanism'' (3,18), whose analysis is one of our major goals in this study.

We recently presented a theoretical approach for modeling the adsorption of charged flexible polymers onto mixed, oppositely charged, fluid membranes (19). We showed there that the Rosenbluth Monte Carlo (MC) scheme for simulating polymer statistics in solution (20,21) can be extended and applied to model the interaction of polymers with multicomponent fluid membranes. This modeling scheme, which we also use in this study, allows and thus explicitly accounts for lipid mobility within the membrane plane, and hence for possible local changes in lipid composition, in response to interactions with nearby peripheral macromolecules (see also (22,23)). In a previous study (19), we described in detail how thermodynamic and configurational characteristics of the polymer-membrane system can be derived from the simulation data, demonstrating the approach for a relatively simple model system; a 20-segment-long positively charged homopolyelectrolyte, interacting with mixed membranes containing neutral, monovalent, and polyvalent acidic lipids. The emphasis there has been on the theoretical-computational background as well as on the differences between polymer binding to fluid versus ''frozen'' membranes and versus uniformly charged surfaces.

The conceptual framework and computational algorithms developed in Tzlil and Ben-Shaul (19) are applied here to study the considerably more complex and biologically more relevant process of MARCKS binding to fluid membranes composed of neutral, monovalent (e.g., PS) and tetravalent (PIP_2) lipids. In addition to simulating the adsorption of our MARCKS (heteroplymeric) model, we also study its phosphorylated isomer, thus modeling the ''myristoyl-electrostatic-switch'' mechanism. A related protein of interest is the mutant MARCKS-FA, in which all the phenylalanines of the MARCKS-ED peptide are replaced by the less hydrophobic alanine residues (10).

Several theoretical-computational studies, including atomic-level binding calculations (4,24,25), statistical-thermodynamic analyses (22,23,26,27), as well as a very recent transfer matrix formulation (28), have addressed some of the questions of interest here, primarily the localization of specific membrane lipids mediated by peripherally bound macromolecules. However, as far as we are aware of, none of these works has explicitly been concerned with the binding of flexible proteins to multicomponent fluid membranes, which constitutes our general goal in this study. Specifically, our detailed simulations of membrane-MARCKS binding are intended to yield new and additional insights into the mechanisms underlying the adsorption of charged, unstructured, proteins onto mixed fluid membranes, with particular emphasis on: i), The role of lipid mobility, especially in connection to PIP_2 sequestration. ii), A detailed examination of the interplay among the various electrostatic, hydrophobic, and entropic contributions to protein-membrane binding. iii), A further examination of the electrostatic switch mechanism as pertains to MARCKS. The simulations analyzed in the next sections, even for our approximate protein-membrane model, are computationally quite demanding. Focusing on the major issues of biophysical interest, we have thus chosen to analyze here the adsorption of MARCKS, its FA mutant, and their phosphorylated isomers, on three representative membranes of interest, corresponding to different proportions of the neutral, monovalent, and tetravalent lipids (PC:PS:PIP_2 = 89:10:1, 99:0:1 and 90:10:0).

THEORY AND SIMULATION MODEL

MARCKS domains

In solution, owing to the electrostatic repulsion between its charged residues, MARCKS-ED (residues 152–176 of MARCKS), like other polyelectrolytes, is expected to be relatively stretched compared to a similarly long uncharged peptide (29,30). Experiment reveals that upon adsorption, the MARCKS-ED assumes an extended conformation (31), which could be even more extended than in the bulk solution due to the additional electrostatic repulsion between the ''neutralizing'' acidic lipids localized in the adsorption zone.

Contrary to the strong attraction of the basic domain to the membrane, the loop (residues 1–151) and tail (177–332) chains emanating from the ED are expected to be repelled from the membrane owing to two mechanisms. The first is entropic, resulting from the lower configurational freedom of the chains due to excluded volume interactions with the membrane surface. Secondly, the chains are moderately acidic and are thus electrostatically repelled from the acidic membrane. (The loop carries 24 negative and 10 positive residues, implying a net charge of $\zeta = -14$, roughly randomly spread along the chain. The corresponding numbers for the tail are −35 and +7, and hence $\zeta = -28$.) As we shall see in the next section, our calculations indicate that the electrostatic repulsion is weaker than that due to excluded volume interactions. They also suggest that these repulsions are not strong enough to modify the extended and ''flat'' configurations of the basic domain due to its strong electrostatic attraction and hydrophobic binding to the membrane. Consequently, since its ED-bound end resides generally near the membrane surface, the tail may be regarded as an end-grafted polymer. The loop is grafted to the membrane at both ends, one connected to the basic domain and the other—the myristoylated N-terminus—hooked to the membrane's hydrophobic core.

As in our previous study, we use here an approximate, ''coarse grained'' model of the protein, treating it as a freely jointed chain of charged, hydrophobic, and neutral beads, according to the amino acid sequence; all beads are of the same diameter d (19,31). The lipid membrane is modeled as a perfectly flat two-dimensional (2D) hexagonal lattice, with lipid headgroups occupying all of its lattice sites. Since the distance between nearest neighbor lipid headgroups is generally comparable to the spacing, d, between amino acid side chains along the protein backbone, we further simplify the model and set the minimal interlipid distance equal to d. In the numerical simulations, we use a membrane lattice constant of $d = 8.66$ Å (corresponding

to a lipid membrane where the area per headgroup is 65 Å^2; see Tzlil and Ben-Shaul (19) for additional details).

The amino-acid sequence of the central basic domain is shown in Fig. 1. This sequence as well as those of the long tail and loop chains were taken from Swiss-Prot database (32). Our MARCKS simulation model accounts in detail for the position and character (charge and degree of hydrophobicity) of the amino acids along the ED. It also accounts for the exact positions of the charged residues along the tail and the loop, but all their other residues (most of which are alanines and prolines) are modeled as identical, electrically neutral, beads. Owing to the substantial computational difficulty of simulating the interaction among the long (332-segment, heteropolymeric) intact MARCKS with the three component fluid membrane, we have separately simulated the conformational statistics and membrane binding characteristics of the loop, of the ED, and of the tail. In other words, we have treated the loop, ED, and tail as noninteracting chains, except for (grafting) boundary conditions imposed on the tail and the loop, as detailed below. This approximation is supported by the notion (later confirmed by our simulations) that the relatively short ED binds strongly, both electrostatically and hydrophobically, to the lipid membrane with all its segments lying nearly flat on its surface. Although linked to the ED, the tail and loop hardly affect the conformational statistics of the adsorbed ED, or the spatial distribution of the lipids in its vicinity.

Another difference between our simulations of ED-membrane versus tail-membrane and loop-membrane simulations involves the treatment of the lipid membrane. Although we explicitly account for lipids' mobility and their redistribution in the membrane upon adsorption of the ED, in simulating the tail and the loop, we model the membrane as a uniformly charged surface, with all lipids carrying the same average partial charge. In this approximation, the tail and the loop experience the same electrostatic potential everywhere across the 2D membrane surface, and their charged residues cannot induce local changes in lipid composition. This ''uniform membrane approximation'' thus sets an upper bound to the electrostatic repulsion energy between membrane and chains. To asses the importance of this interaction, we have carried out additional simulations in which all chain segments are electrically neutral. Detailed results will be given in subsequent sections, yet we can mention that the neutral and charged chains reveal very similar behaviors and just a small difference in chain-membrane repulsion energy (~1 kcal/mole), supporting our approximate treatment of loop-membrane and tail-membrane interactions.

The boundary conditions imposed on the loop and the tail are: i), The first segment of the loop (corresponding to the myristoylated N-terminus) is always found at the membrane's plane. ii), The last (151th) segment of the loop is kept fixed at the (average) position of the first (152th) ED segment, i.e., very close to the membrane's surface. iii), The position of the first (177th) tail's segment is fixed at the (average) position of the last (176th) ED residue. As argued above, subject to these boundary conditions, the protein-membrane binding free energy can be expressed as a sum of three contributions,

$$\Delta F = \Delta F_{\mathrm{ED}} + \Delta F_{\mathrm{loop}} + \Delta F_{\mathrm{tail}}, \tag{1}$$

with each term representing the difference between the free energy of the corresponding domain in its adsorbed state and as a free polymer in solution. Note that ΔF is essentially ''the standard free energy of adsorption'', and thus does not include the loss of translational entropy of the (''united'') protein upon binding. The change in translational entropy depends, of course, on peptide concentration and affects the adsorption isotherms and related properties; as discussed in the next section.

The tail's contribution to ΔF is

$$\Delta F_{\mathrm{tail}} = \Delta E_{\mathrm{tail}} - T\Delta S_{\mathrm{tail}}, \tag{2}$$

where the first term accounts for the electrostatic repulsion from the membrane, whereas the second (and as it turns out, more important) term reflects the loss of conformational entropy experienced by the tail upon grafting its first segment to the membrane. Similarly,

$$\Delta F_{\mathrm{loop}} = \Delta E_{\mathrm{loop}} - T\Delta S_{\mathrm{loop}} + \Delta E_{\mathrm{myr}}, \tag{3}$$

involves an electrostatic repulsion term and a conformational entropy loss term that now accounts for grafting both ends of the loop. The hydrophobic insertion energy of the myristoylated N-terminal anchor, ΔE_{myr}, provides the largest contribution to the loop's binding free energy.

The myristoyl insertion free energy has been estimated experimentally as $\Delta F_{\mathrm{myr}} \approx -8\,\mathrm{kcal/mole} = -13.5\,k_{\mathrm{B}}T$ (3), where k_{B} is Boltzmann's constant and T is the absolute temperature. This estimate is based on measurements of the partitioning of a short end-myristoylated peptide, comprising the first 15 groups of the Src protein, between solution and an electrically neutral lipid membrane. Besides the hydrophobic interaction of the myristoyl chain, ΔF_{myr} includes the loss of conformational freedom experienced by the rest of the peptide upon adsorption. For a freely jointed chain of length N, the corresponding entropy loss is estimated theoretically as $\Delta S = k_{\mathrm{B}}\ln\sqrt{N}$ (33), so that for the above peptide $-T\Delta S = 0.5\ln 15 = 1.35\,k_{\mathrm{B}}T$. We have also estimated this entropy loss based on our MC simulation scheme and found $-T\Delta S = 1.7\,k_{\mathrm{B}}T$. Using this latter estimate, we conclude that $\Delta E_{\mathrm{myr}} = -13.5 - 1.7 = -15.2\,k_{\mathrm{B}}T$, and later employ this value in our calculations.

Interaction potentials

The basic residues of the MARCKS-ED peptide (12 lysines, K in Fig. 1, and one arginine, R) are represented in our model by spherical beads with a unit positive charge in their center. The tail and the loop are modeled as freely

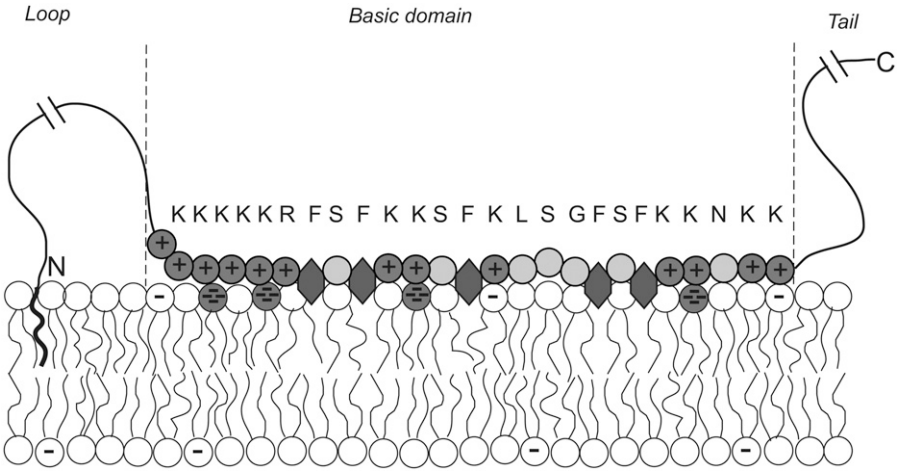

FIGURE 1 Schematic representation of an adsorbed MARCKS protein. Circles enclosing the + symbol and open circles denote basic and electrically neutral amino acids, respectively. The hydrophobic phenyl groups that tend to insert into the membrane's hydrophobic core are represented by hexagons. Also illustrated are neutral and several acidic lipid headgroups, represented by circles enclosing one (e.g., monovalent PS) or four (tetravalent PIP_2) negative charges. The amino acid sequence of the basic domain is shown explicitly. For the long tail and loop sequences (not shown) see, e.g., Swiss-Prot database (32).

jointed chains of beads (all of diameter d), carrying acidic, basic, and neutral residues, as dictated by the known amino acid sequences of these chains. For comparison, we have also calculated the energetic and conformational properties of equally long tail and loop chains comprising only neutral beads.

Upon adsorption, MARCKS-ED acquires an extended conformation and the binding is enhanced by the insertion of the five phenylalanines (F) into the membrane's hydrophobic core (31). These residues are represented by spherical beads that can partly penetrate the hydrophobic core. A similar model is used for the more weakly binding leucine (L) residue. In certain control experiments, the phenylalanines of MARCKS-ED were substituted by alanines (A); the corresponding peptide is known as MARCKS-FA-ED. The experiments showed that this substitution reduces substantially the extent of PIP_2 sequestration. To compare our simulations to these experiments, we shall model this peptide using a weaker hydrophobic interaction potential, as detailed below.

As noted earlier, MARCKS detaches from the membrane upon phosphorylation of three serine (S) groups residing in its ED, reducing its net charge from +13 to +7. We shall model the phosphorylated state of MARCKS-ED by assigning a charge of $\zeta = -2$ to the three serine residues located in the centers of the corresponding beads. We now turn to a more detailed description of the various potentials used.

Excluded volume interactions

There are no restrictions in our model on the angles between successive bonds along the polymers representing the three protein domains, but we do account for excluded volume interactions between (all pairs of) nonbonded chain segments. This short-ranged repulsion is modeled using the truncated and shifted Lennard-Jones potential:

$$u_{\mathrm{LJ}}(r) = \begin{cases} 4\varepsilon[(\sigma/r)^{12} - (\sigma/r)^{6}] + \varepsilon & \text{if} \quad r \geq 2^{1/6}\sigma \\ 0 & \text{if} \quad r \leq 2^{1/6}\sigma \end{cases}. \quad (4)$$

We set $2^{1/6}\sigma = d$ and $\varepsilon = 0.1\,k_{\mathrm{B}}T$, thus ensuring the onset of steep repulsion as soon as r falls below d (34).

The membrane surface is treated as an impenetrable wall to all the polar protein groups, implying a minimal distance of $d/2$ between polymer and lipid charges. The (centers of the) hydrophobic residues (Phe, Ala, and Leu) are allowed to penetrate the membrane interface down to $z = 0$, as described below.

Electrostatic interactions

The charged amino acids are treated as spherical beads with point charges residing in their centers. Similarly, the charged lipids are treated as disks bearing point charges at their centers. Although the charged residues of MARCKS-ED are always located in the aqueous region, they generally reside very near the membrane-water interface. This is due to the electrostatic attraction of the basic residues to acidic membrane lipids, as well as to their pulling toward the membrane by the membrane-inserted phenylalanines (31).

To account for the proximity of the protein charges to the membrane-water interface, we use here a recent extension of Debye-Hückel (DH) theory due to Netz (35), in which the presence of a dielectric discontinuity is explicitly taken into account. Closed-form expressions for the modified DH potentials are available for geometries such as the membrane-water interface in which the dielectric constant on one side of the boundary (i.e., the hydrophobic membrane core) is negligible compared to that of the other side (the aqueous solution). The interaction potential between two ionic charges q and q' at distance r apart, located at distances z and z', respectively, from the interface is then given by (35)

$$u_{\mathrm{DH}}(r, z, z') = qq' l_{\mathrm{B}} \frac{e^{-\kappa r}}{r} + qq' l_{\mathrm{B}} \frac{e^{-\kappa\sqrt{r^2 + 4zz'}}}{\sqrt{r^2 + 4zz'}}. \quad (5)$$

In Eq. 5 and hereafter, unless otherwise specified, the interaction potentials and all other energies are measured in units of $k_{\mathrm{B}}T$, and distances will be measured in units of d. $l_{\mathrm{B}} = e^2/\varepsilon k_{\mathrm{B}}T$ is the Bjerrum length where e is the elementary charge and ε is the dielectric constant of water, and κ^{-1} is the Debye screening length. In all calculations, we use $l_{\mathrm{B}} = 7.14$ Å, appropriate for water at room temperature, and $\kappa^{-1} = 10$ Å, which corresponds to typical physiological conditions (monovalent ionic strength of ~0.1 M). Notice that at the interface($z = z' = 0$), the interaction becomes twice as large as the interaction with no dielectric boundary. We shall use Eq. 5 for all relevant electrostatic interactions, i.e., between protein charges, membrane charges and membrane-protein charges.

We also account for the effect of a nearby dielectric boundary on the Born self-energy, (assuming, as in Eq. 5, that the dielectric constant within the membrane is negligible compared to that of water). Explicitly, the charging energy of an ion of charge q located at a distance z from the membrane, relative to its value in solution, is given by (35)

$$u_{\mathrm{DH}}^{\mathrm{self}}(z) = \frac{q^2}{2} l_{\mathrm{B}} \frac{e^{-2\kappa z}}{2z}. \quad (6)$$

Note that this excess Born energy implies an effective repulsion of the ionic charges from the membrane.

The assumption underlying Eqs. 5 and 6, that a sharp boundary separates the high (water) and low (hydrocarbon membrane core) dielectric media, is, of course, an approximation. The hydrocarbon-water interface, containing the various lipid headgroups, is of nonzero thickness and its ''effective'' dielectric constant is intermediate between those of water (~80) and of the membrane interior (~2). Furthermore, it is inhomogeneous and depends on lipid composition. In using Eqs. 5 and 6, we assume that the effect of this narrow interfacial shell on electrostatic interactions in the aqueous region is small compared to those implied by the presence of an infinite low dielectric medium beyond the interface boundary.

Hydrophobic interactions

Our model allows the hydrophobic residues to partly penetrate into the membrane's hydrophobic core. To this end, we use simplified square-well-like potentials for all hydrophobic residues. We determine their depth, D_{h}, so as to reproduce the molar partition coefficient of the relevant amino acid, as measured by Wimley and White (for specific peptides interacting with neutral membranes) (36). Explicitly, the hydrophobic amino acids are allowed to insert down to distance $d/2 \simeq 4.3$ Å, (corresponding, roughly, to the size of a phenyl group), and their interaction potential with the membrane is given by

$$u_{\mathrm{h}}(z) = \begin{cases} \infty & z < 0 \\ -D_{\mathrm{h}} & 0 \leq z \leq d/2 \\ 0 & z > d/2 \end{cases}. \quad (7)$$

Using our simulation scheme to model the partition coefficients of the peptides studied by Wimley and White (36), we derived the following well depth values: $D_{\mathrm{h,leu}} = 2.4\,k_{\mathrm{B}}T$, $D_{\mathrm{h,ala}} = 0.7\,k_{\mathrm{B}}T$, and $D_{\mathrm{h,phe}} = 3.5\,k_{\mathrm{B}}T$. Additional details are given in Appendix A.

It should be noted that we neglect hydrophobic interactions due to the membrane penetration of hydrophobic residues in the loop and tail regions, because neither region contains an appreciable local density of hydrophobic residues, and because entropic and electrostatic repulsions are expected to outweigh any potential hydrophobic contributions.

Thermodynamic and structural properties

From the simulations, we derive both structural characteristics of the protein-membrane system, e.g., dimensions of the adsorbed protein and thermodynamic properties such as adsorption free energies and their various components. The theoretical-computational background underlying these calculations

has been described in our earlier work (19). Skipping most details of the computational algorithm, we briefly outline below the basic physical assumptions of our thermodynamic model and the procedures used to derive structural and thermodynamic averages of interest.

Thermodynamic model

We find it computationally convenient to classify the (numerous) configurations of the macromolecule-membrane system according to the position of a particular polymer segment (or, alternatively, the center of mass) from the membrane plane. Quite arbitrarily, we have chosen to classify these configurations according to the distance, z_1, of the first (equivalently, the last) polymer segment from the membrane. We use

$$q(z_1) = \sum_{m,\alpha} \exp[-U(m,\alpha|z_1)] \tag{8}$$

to denote the partition function of an adsorbed macromolecule with a given z_1, where $U(m,\alpha|z_1) = U(m) + U(\alpha|m,z_1)$ is the potential energy corresponding to a specific membrane-polymer configuration; $U(\alpha|m,z_1)$ denotes the energy of a polymer in conformation α, whose first segment is fixed at distance z_1 from the membrane plane, interacting with a membrane in a given lipid configuration m. $U(\alpha|m,z_1)$ includes the self-energy of the polymer (i.e., the sum of its intersegment potentials), as well as its interaction energy with the membrane. $U(m)$ is the interlipid interaction energy.

All simulations involving the MARCKS-ED peptide refer to its adsorption on mixed ''fluid'' (as opposed to ''frozen'') membranes. The various lipid species comprising a fluid membrane are laterally mobile and can thus adjust their local composition in response to interactions with peripheral molecules. In particular, the highly basic MARCKS-ED is expected to sequester acidic lipids, especially PIP_2 molecules, localizing them to its immediate vicinity. On the other hand, as noted above, the electrostatic interaction of the (very long and sparsely charged) tail and loop chains with the membrane is rather weak. Consequently, their tendency to modify the 2D distribution of the acidic lipids is much weaker. Thus, in simulating their interaction with the membrane surface, we use a simpler, ''uniform membrane'' model, whereby the total membrane charge is evenly shared among all its constituent lipids, corresponding essentially to a homogeneously charged planar surface with a uniform surface potential. Note that the uniform membrane involves only one lipid configuration and the sum over m in Eq. 8 is, of course, redundant. It should be understood that all the forthcoming equations that involve summation over m refer to fluid membranes; the uniform membrane may be regarded as a (degenerate) special case.

We use λ to denote the thickness of the adsorbed layer, defined here as the distance ($z_1 > \lambda$) from the membrane surface beyond which ΔF practically vanishes. (Alternative definitions can be given, e.g., in terms of the surface excess (19).) The average partition function of an adsorbed macromolecule is thus

$$q^{(1)} = (1/\lambda)\int_0^{\lambda} q(z_1)dz_1. \tag{9}$$

For $z_1 > \lambda$, the polymer no longer interacts with the membrane, and hence $U(m,\alpha|z_1) = U(m) + U(\alpha)$. In this limit $q(z_1 > \lambda) = q(\infty) = q^{(0)}q_b$, where

$$q^{(0)} = \sum_m \exp[-U(m)] \tag{10}$$

is the partition function of the free membrane, and

$$q_b = \sum_{\alpha} \exp[-U(\alpha)] \tag{11}$$

is the conformational partition function of the macromolecule (with its first segment fixed at some arbitrary point) in the bulk solution.

The thermodynamics of protein adsorption on a fluid membrane is adequately described in terms of a simple lattice model, as follows. The lipid membrane, of total area A, is regarded as a 2D array of $M = A/a$ noninteracting cells, all of the same area, a, and of the same lipid composition, each cell capable of accommodating one adsorbed macromolecule. We may also assign a volume to these adsorption cells, $\nu = a\lambda$, where λ is the thickness of the surface layer. The membrane is in equilibrium with a bulk solution of volume V containing N_P macromolecules. Consistent with modeling the surface layer as a 2D lattice, we treat the bulk solution as a three-dimensional array of V/ν cells. Assuming dilute solution behavior, the chemical potential of the macromolecules is then given by $\mu = -\ln q_b + \ln\varphi$, where $\varphi = N_P\nu/V$ is the volume fraction of macromolecules in solution.

Treating the membrane as an open system with respect to macromolecule exchange, the grand-canonical partition function of our model system above is

$$\Xi_f = (\xi)^M = [q^{(0)} + \gamma q^{(1)}]^M, \tag{12}$$

where $\gamma = \varphi/q_b = \exp(\mu)$ is the absolute activity, and $\xi = q^{(0)} + \gamma q^{(1)}$ is the two-state (empty and occupied) partition function of one membrane cell. Using N_{LP} to denote the number of adsorbed macromolecules, the fraction of occupied cells (or the ''surface coverage'') is $\theta = N_{LP}/M = N_{LP}(a/A)$. From the thermodynamic relationship $N_{LP} = \partial\ln\Xi/\partial\mu = \partial\ln\Xi/\partial\ln\gamma$, it then follows that $\theta = \gamma q^{(1)}/\xi$, yielding the Langmuir-like adsorption isotherm

$$\frac{\theta}{1-\theta} = \frac{\gamma q^{(1)}}{q^{(0)}} = \varphi\frac{q^{(1)}}{q_b q^{(0)}} = \varphi e^{-\Delta F}, \tag{13}$$

where

$$\Delta F = -\ln(q^{(1)}/q_b q^{(0)}) \tag{14}$$

is the adsorption free energy, per macromolecule.

From the MC simulations we derive q_b, $q^{(0)}$, and all the $q(z_1)$ values, using which we calculate $q^{(1)}$ (Eq. 9) and the adsorption free energy ΔF (Eq. 14). Similarly, the statistical average, $\langle A\rangle$, of any thermodynamic or structural property of the adsorbed macromolecule can be calculated using

$$\langle A\rangle = \int_0^{\lambda} q(z_1)\langle A(z_1)\rangle dz_1 \Big/ \int_0^{\lambda} q(z_1)dz_1. \tag{15}$$

Partition coefficients

The adsorption-free energies derived from the simulations can be related to experimentally measurable molar partition coefficients, $K_a = [LP]/[L][P]$, where $[LP]$, $[L]$ and $[P]$ are, respectively, the concentrations of lipid-protein complexes (i.e., adsorbed proteins), total lipid, and free protein in solution. Expressing these concentrations in terms of the number of molecules (N_{LP}, etc.), we have

$$[LP] \equiv N_{LP}/V;\ [P] \equiv N_P/V = \varphi/\nu;\ [L] \equiv N_L/V = (A/a_L)/V, \tag{16}$$

where a_L (typically $\sim$65 Å^2) is the average cross-sectional area per lipid headgroup. For low concentrations of proteins in solution ($\varphi = N_P\nu/V \ll 1$), and correspondingly small values of membrane coverage ($\theta = N_{LP}a/N_L a_L \ll 1$), Eq. 13 yields $\theta = \varphi\exp(-\Delta F)$, and hence

$$K_a = \frac{[LP]}{[L][P]} = \lambda a_L \frac{q_f^{(1)}}{q_b q^{(0)}} = \lambda a_L e^{-\Delta F}. \tag{17}$$

To compare our calculations with experimentally determined K_a values, we note that ΔF is measured here in k_BT values, and that λa_L is a molecular volume, (e.g., for a typical membrane layer thickness of $\lambda = 10\,d = 86.6$ Å and lipid area of 65 Å^2, we have $\lambda a_L \simeq 5630$ Å^3). Experimentally measured ΔF values are generally expressed in kcal/mole (1 kcal/mole $\simeq 0.6\,k_BT$ at

room temperature), and the concentrations, e.g., $[P]$, in moles per liter, so that the units of K_a are $[M]^{-1}$. For the representative value of λa_L above, we find $K_a([M]^{-1}) = 3.39 \times \exp(-\Delta F\,(\text{kcal/mole})/0.6)$.

RESULTS AND DISCUSSION

Several series of MC simulations were carried out for MARCKS, its MARCKS-FA mutant (where the five phenylalanines of the ED are replaced by alanines) and their phosphorylated isomers (where the net charge on the ED is +7 rather than +13). Results are presented for the MARCKS-ED peptide as well as for the intact MARCKS. Focusing mainly on the role of PIP_2 lipids in MARCKS-membrane interaction, we have chosen three representative membrane compositions:

i. A binary, PC:PS = 90:10, membrane containing 90% neutral (e.g., phosphatydylcholine, PC) lipids and 10% monovalent acidic (e.g., PS) lipids. (Typical concentrations of PS in biomembranes are 10–30%).
ii. A ternary membrane, PC:PS:PIP_2 = 89:10:1, containing neutral, monovalent, and 1% tetravalent PIP_2 lipids, corresponding to typical physiological concentrations.
iii. A PC:PIP_2 = 99:1 membrane, which contains 1% PIP_2 lipids but no PS. This last case is of interest for comparative purposes, as well as because it has been studied experimentally as a special model system.

All simulations were carried out for a single protein domain (the effector domain, the tail or the loop) interacting with a 50 × 50 hexagonal membrane cell, with periodic boundary conditions. This membrane cell is large enough to accommodate each of the adsorbed macromolecules studied. (Note that the spatial dimensions of the tail and the loop are $\sim\sqrt{150} < 12$; ED is, of course, smaller.) In all cases, the simulations ran over no less than 1 million MC steps, thus ensuring good convergence of the binding free energies and their components. More specifically, this ensured convergence to within a fraction of a percent for the PS containing membranes, and to within about 1% for the PC:PIP_2 = 99:1 membrane. As explained in the previous section, thermodynamic and structural data (for MARCKS-ED and its isomers) were calculated by integrating the results of simulations corresponding to different values of z_1, with z_1 sampled in steps of $\Delta z_1 = d/2$.

Structural properties

Fig. 2 shows two typical simulation snapshots of MARCKS-ED adsorbed on a fluid membrane, exhibiting its tendency to stretch along the membrane surface, with the phenyl side chains inserted into the hydrophobic core. Also apparent is the localization of PIP_2 lipids to the vicinity of the adsorbed peptide. Not entirely obvious from the two snapshots depicted in Fig. 2, but clearly revealed by our quantitative calculations (as described in more detail below), is that the presence of monovalent PS lipids in the membrane hardly affects the sequestration of PIP_2. To demonstrate the role of the phenyl residues in stretching MARCKS-ED parallel to the membrane plane, we show in Fig. 3 the distribution, $P(z)$, of chain segments along the membrane normal, for MARCKS-ED and MARCKS-FA-ED in their adsorbed state. This distribution is calculated using

$$P(z) = \int_0^{\lambda} q(z_1)n(z|z_1)dz_1 \Big/ N\int_0^{\lambda} q(z_1)dz_1, \qquad (18)$$

where $n(z|z_1)dz$ is the average number of polymer segments located between z and $z + dz$, given that the first segment is fixed at z_1; $N = \int_0^{\infty} n(z|z_1)dz$ is the total number of polymer segments (19). The figure shows very clearly that owing to the anchored phenyl groups, MARCKS-ED lies flat on the membrane, whereas the less hydrophobic peptide MARCKS-FA-ED extends significantly toward the aqueous medium.

Lipid redistribution

Let $\psi_i(r)$ denote the local concentration of lipid species i, at distance r from the center of the polymer's adsorption zone, i.e., from the projection of the average center of mass position onto the membrane plane. The (differential) enrichment factor of lipid species i is defined as the ratio $\psi_i(r)/\psi_0^{(i)}$ between its local concentration and its average membrane concentration $\psi_0^{(i)}$, reflecting the extent to which the adsorbed protein sequesters the lipid i (19,37). In Fig. 4, we show the enrichment factor of i = PS and PIP_2 lipids for MARCKS-ED and MARCKS-FA-ED and their phosphorylated isomers, when adsorbed on any of the three types of membranes considered here. We note that the concentration of PIP_2 within the interaction zone (extending from $r = 0$ to $r \sim 6$) is significantly higher than its average membrane value. On the

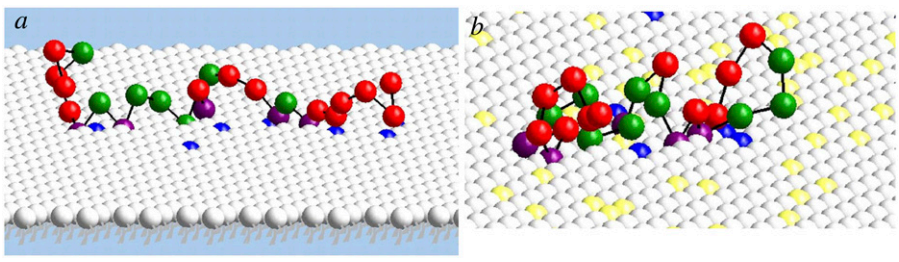

FIGURE 2 Typical simulation snapshots of MARCKS-ED adsorbed on a PC:PIP_2 = 99:1 membrane (*a*), and on a PC:PS:PIP_2 = 89:10:1 membrane (*b*). Red and green spheres represent positively charged and neutral amino acids, respectively. Purple beads denote the hydrophobic phenylalanines. PIP_2, PS, and PC lipids are represented by blue, yellow, and white spheres, respectively. Notice the insertion of the phenyl groups into the lipid membrane and the localization of PIP_2 lipids to the polymer vicinity.

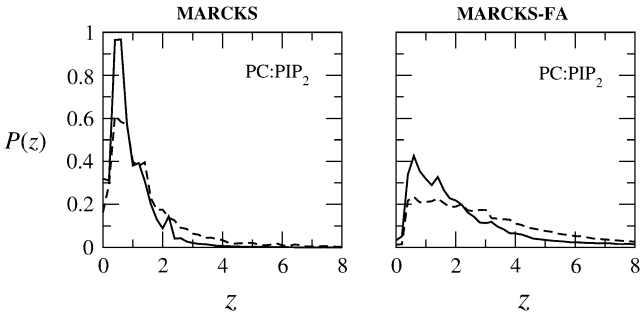

FIGURE 3 Segment distribution along the membrane normal of adsorbed MARCKS-ED (*left*) and MARCKS-FA-ED (*right*), as a function of the distance z (in units of d) from the membrane surface. The solid and dashed curves correspond, respectively, to the nonphosphorylated and phophorylated isomers. All results are for the PC:PIP_2 = 99:1 membrane. (Similar results were obtained for the PC:PS:PIP_2 = 89:10:1 membrane.)

other hand, PS enrichment is negligible in all cases. A detailed explanation to this behavior was given in our previous work (19). Qualitatively, the difference is due to the fact that the mixing entropy loss associated with the transfer of four PS lipids from the bulk of the membrane into the interaction zone is much larger than the demixing entropy penalty inflicted by the transfer of one tetravalent PIP_2 molecule. The contribution of both processes to electrical neutrality is, of course, the same. Interestingly, a very recent theoretical study, dealing with the lateral diffusion of charged basic peptides (e.g., MARCKS-ED) on a mixed lipid membrane containing oppositely charged mono- and multivalent lipids arrives at similar conclusions, though from a different—kinetic—viewpoint (38). Explicitly, this dynamic mean-field study indicates that the peptide sequesters and strongly binds the multivalent lipids, diffusing with those ''bound lipids'' as an ''inseparable'' cluster. The monovalent lipids, on the other hand, bind only weakly and transiently, and cannot follow the motion of the cluster. Their lateral distribution in the membrane is thus barely affected by the adsorbed protein, consistent with our observation regarding the enrichment factor of mono- versus multivalent lipids (Fig. 4). It should be stressed, however, that highly charged macromolecules adsorbed on moderately (oppositely) charged membranes can induce substantial modulations of lipid charge, even if the constituent lipids are monovalent; see, e.g., Harries et al. (22).

The average number of PIP_2 molecules within the interaction region is given by $n_{PIP_2} = \int \psi_{PIP_2}(r) 2\pi r dr$. Integrating over the local PIP_2 concentration we find that $n_{PIP_2} \cong 4$ PIP_2 lipids are sequestered per one adsorbed MARCKS-ED peptide, comparable to the values known from experiment (9,39). The calculated enrichment factor for the MARCKS-FA-ED peptide is somewhat smaller, ~3 PIP_2 per adsorbed peptide. Note, however, that we also find a lower binding free energy for MARCKS-FA-ED as compared to MARCKS-ED, resulting (for the same bulk concentrations) in a smaller number of adsorbed peptides (see below).

Fig. 5 shows $\rho(r)$, the radial distribution of MARCKS-ED segments. As expected, the lateral dimensions of the polymer ($r_{max} \sim 6$) correlate closely with the dimensions of the region enriched by charged acidic lipids. We also note that the extent of this region is not affected by phosphorylation, which is not surprising because phosphorylation dramatically reduces the number of adsorbed peptides (see below), but hardly affects

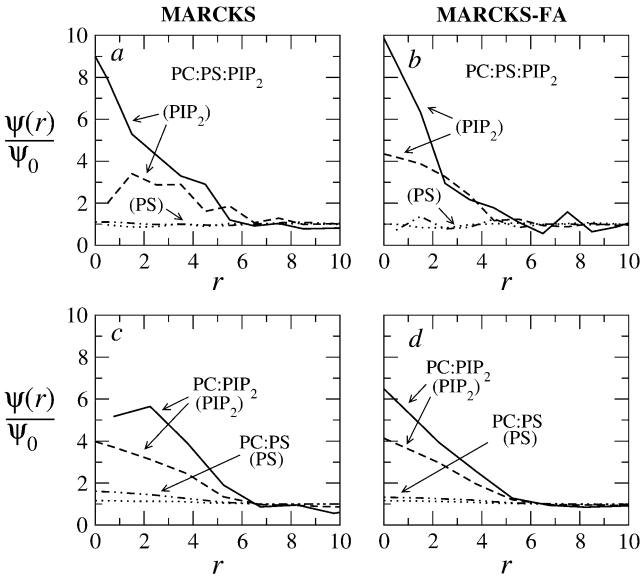

FIGURE 4 Enrichment factor of charged lipids as a function of the radial distance from the (membrane projection of the) protein's center of mass. Results are shown for MARCKS-ED (*a* and *c*) and MARKCS-FA-ED (*b* and *d*) adsorbed on the PC:PS:PIP_2 = 89:10:1 membrane (*a* and *b*), and the PC:PS = 90:10 and PC:PIP_2 = 99:1 membranes (*c* and *d*). The arrows indicate the lipid species enriched and the type of membrane considered; e.g., ''PC:PS (PS)'' labels the enrichment of PS lipids in the PC:PS = 90:10 membrane. The solid and dashed (PIP_2) curves correspond to the nonphosphorylated and phophorylated isomers, respectively. The dashed-dotted and dotted curves correspond to the (minor) enrichment of PS by these isomers.

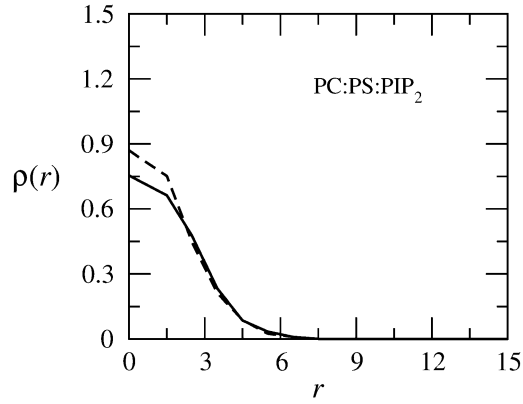

FIGURE 5 Surface density of chain segments as a function of the radial distance from the protein's center of mass. The solid and dashed curves correspond to the nonphosphorylated and phosphorylated MARCKS-ED isomers, respectively. Results are shown only for the PC:PS:PIP_2 = 89:10:1 membrane. Similar results were obtained for the other membranes.

the dimensions of those which remain bound to the membrane.

In Fig. 6, we show a typical spatial configuration of the intact MARCKS on the lipid membrane. The snapshot is, in fact, a superposition of three separate snapshots, corresponding to the ED, tail, and loop domains, tailored together at their appropriate boundaries. In this particular case, the tail and loop were modeled as neutral chains, yet it should be noted that charged chain configurations appear very similar. The similar configurational statistics of the charged and neutral chains are in line with the notion above that membrane-chain repulsion is primarily due to excluded volume (rather than electrostatic) interactions.

Binding free energies

In this section, we present the calculated binding free energies of MARCKS, MARCKS-ED, and their FA mutants, both before and after phosphorylation, all for our three representative membrane compositions. The major results are summarized in Table 1, which lists also the relevant energetic and entropic contributions to the ΔF values. Comparisons with some available experimental results are presented and analyzed.

As argued with regard to Eq. 1, expressing ΔF as a sum of contributions arising from the loop, tail, and effector domains is generally a good approximation. By adopting this scheme, we cannot examine possible intramolecular interactions between the different MARCKS domains, as suggested by some authors (40). Also, this approximation might be less appropriate for strongly acidic membranes, in which case the moderately acidic tail and loop chains may experience strong electrostatic repulsion from the membrane, which, in turn, could (''nonadditively'') interfere with the configurational and energetic behavior of the basic domain. However, for the physiologically relevant membrane compositions of interest here, our calculations suggest that such coupling between the ED and the two flexible chains is quite unlikely. Good qualitative and reasonable quantitative agreement between the predictions of our simulations and available experimental results provides additional support to the validity of Eq. 1. To substantiate these remarks, we begin our analysis with the loop and tail free energies. Recall that we simulate their adsorption using the uniformly charged membrane model, and that the first tail segment and both ends of the loop are grafted to the membrane. More precisely, being chemically connected to the ED, the first segment of the tail (residue 177 of MARCKS) is kept fixed at distance d from the membrane, which corresponds to the average position $\langle z_{25}^{\mathrm{ED}} \rangle \approx d$, of the last ED segment (residue 176) . A similar boundary condition is imposed on the last segment of the loop; its first segment is bound to the membrane through the myristoyl anchor.

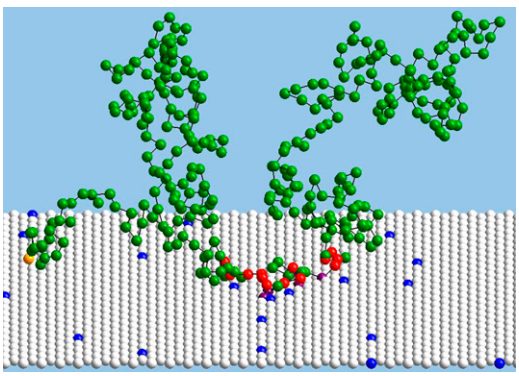

FIGURE 6 Typical snapshot of the MARCKS protein model, demonstrating the extended configurations of the long ''tail'' and ''loop'' domains, as distinguished from the membrane bound central basic domain. Green and red spheres represent here neutral and positively charged amino acids, respectively. The myristoyl anchor is represented by a yellow sphere. PIP_2, PS, and PC lipids are represented by blue, purple, and white spheres, respectively. (In this particular snapshot, the tail and loop chains are electrically neutral. Charged chain configurations appear similarly extended.)

Tail and loop contributions

In the Theory section, we have estimated the myristoyl insertion energy as $\Delta E_{\mathrm{myr}} = -15.2\,k_{\mathrm{B}}T = -9.1\,\mathrm{kcal/mole}$, providing a substantial contribution to the binding energy of the intact protein. Opposite contributions to the binding free energy arise from the repulsive, excluded volume and electrostatic, interactions of the tail and loop chains with the membrane. Our simulations show that their sum, $\Delta E_{\mathrm{tail+loop}}^{\mathrm{elec}} - T(\Delta S_{\mathrm{tail}} + \Delta S_{\mathrm{loop}})$, is typically approximately equal to $|\Delta E_{\mathrm{myr}}|$, thus largely reducing the overall contribution, $\Delta F_{\mathrm{tail+loop}} = \Delta E_{\mathrm{myr}} + \Delta E_{\mathrm{tail+loop}}^{\mathrm{elec}} - T(\Delta S_{\mathrm{tail}} + \Delta S_{\mathrm{loop}})$, of the tail and loop domains to the binding free energy; e.g., for the (relatively strongly charged) PC:PS:PIP_2 = 89:10:1 membrane we found $\Delta E_{\mathrm{tail+loop}}^{\mathrm{elec}} - T(\Delta S_{\mathrm{tail}} + \Delta S_{\mathrm{loop}}) = 7.5\,\mathrm{kcal/mole}$, and hence $\Delta F_{\mathrm{tail+loop}} = -9.1 + 7.5 = -1.6\,\mathrm{kcal/mole}$.

Table 1 reveals that $\Delta E_{\mathrm{tail+loop}}^{\mathrm{elec}} - T(\Delta S_{\mathrm{tail}} + \Delta S_{\mathrm{loop}}) = \Delta F_{\mathrm{tail+loop}} - \Delta E_{\mathrm{myr}}$ is rather similar for the three types of membranes, even though their average charges are quite different. This implies that the contribution to tail and loop repulsion associated with the loss of configurational chain entropy, $(-T(\Delta S_{\mathrm{tail}} + \Delta S_{\mathrm{loop}}))$, is considerably larger than that due to direct electrostatic repulsion $(\Delta E_{\mathrm{tail+loop}}^{\mathrm{elec}})$. This conclusion is further supported by our additional simulations in which all tail and loop segments were modeled as being electrically neutral, in which case $\Delta E_{\mathrm{tail+loop}}^{\mathrm{elec}} \equiv 0$. Here, for all membranes, we found $T(\Delta S_{\mathrm{tail}} + \Delta S_{\mathrm{loop}}) = 5.7$ kcal/mole, yielding $\Delta F_{\mathrm{tail+loop}} = T(\Delta S_{\mathrm{tail}} + \Delta S_{\mathrm{loop}}) - \Delta E_{\mathrm{myr}} = 5.7 - 9.1 = -3.4$ kcal/mole, only 1.8 kcal/mole smaller than its value (−1.6 kcal/mole) for the strongly charged membrane (see Table 1). The difference between these two values represents the direct electrostatic repulsion energy of (both) the tail and the loop from the membrane, indicating that its contribution to ΔF is indeed small. This justifies the assumption embodied in Eq. 1 regarding the additive contributions to ΔF of the three protein domains.

TABLE 1 Adsorption free energies and their various components, for MARCKS-ED, MARCKS-FA, and their phosphorylated ("Phos") isomers on PC:PS:PIP_2 = 89:10:1, 90:10:0, and = 99:0:1 membranes

		PC:PS:PIP_2 = 89:10:1		PC:PIP_2 = 99: 1		PC:PS = 90:10	
		Nonphos	Phos	Nonphos	Phos	Nonphos	Phos
MARCKS	ΔF	−9.1	−5.3	−7.2	−4.8	−4.3	−2.7
	ΔF_{ED}	−7.5	−3.7	−4.6	−2.2	−2.7	−1.1
	ΔE_{ED}	−25.5	−18.0	−24.4	−14.5	−12.5	−6.7
	$T\Delta S_{ED}$	−18	−14.3	−19.8	−12.3	−9.8	−5.5
	$K_a^{ED}[M^{-1}]$	2×10^6	3×10^3	2×10^4	2×10^2	4×10^2	3×10^1
	$\Delta F_{tail+loop}$	−1.6 (−3.4)	−1.6(−3.4)	−2.6 (3.4)	−2.6(−3.4)	−1.6 (−3.4)	−1.6(−3.4)
	$\Delta E_{elec(+Leu)}$	−17.3	−12.9	−16.8	−9.3	−5.8	−2.7
	ΔE_{Born}	0.4	0.8	0.5	0.6	0.3	0.4
	ΔE_{Phe}	−8.6	−5.9	−8.1	−5.8	−7.0	−4.4
	n_{PIP_2}	3.65	2.97	4.45	2.8	0	0
MARCKS-FA	ΔF	−5.4	−3.4	−3.8	−3.3	−2.5	−2.0
	ΔF_{ED}	−3.8	−1.8	−1.2	−0.7	−0.9	−0.4
	ΔE_{ED}	−15.0	−8.8	−9.5	−5.8	−2.6	−1.2
	$T\Delta S_{ED}$	−11.2	−7.0	−8.3	−5.1	−1.7	−0.8
	$K_a^{ED}[M^{-1}]$	4×10^3	1×10^2	4×10^1	1×10^1	8	4
	$\Delta F_{tail+loop}$	−1.6 (−3.4)	−1.6(−3.4)	−2.6 (3.4)	−2.6 (3.4)	−1.6 (−3.4)	−1.6(−3.4)
	$\Delta E_{elec(+Leu)}$	−15.1	−9.0	−9.6	−6.0	−2.6	−1.3
	ΔE_{Born}	0.4	0.2	0.3	0.2	0.1	0.1
	ΔE_{Ala}	−0.3	−0.05	−0.2	−0.05	−0.1	−0.01
	n_{PIP_2}	3.08	2.63	3.5	2.5	0	0

ΔE_{Phe} and ΔE_{Ala} are the contributions due to the hydrophobic insertion of (all) the phenylalanine and alanine residues, respectively. ΔE_{Born} is the Born self-energy and $\Delta E_{elec} = \Delta E - \Delta E_{Phe/Ala} - \Delta E_{Born}$ is the electrostatic contribution to the binding. (The small contribution of the single leucine residue is not included in the Phe/Ala contribution but rather added to the electrostatic energy). n_{PIP_2} is the number of PIP_2 lipids sequestered into the adsorption region. The number in parenthesis (−3.4) for $\Delta F_{tail+loop}$ is the value obtained for electrically neutral tail and loop chains. All energies in kcal/mole.

A noteworthy result of the simulations is that for the electrically neutral chains, $\Delta S_{loop} \approx 3\Delta S_{tail}$, which is not very surprising considering that the tail is grafted to the membrane at one end whereas the loop is grafted at both ends. Interestingly, the value derived from the simulations, $T\Delta S_{tail} \approx (5.7/4)\,\text{kcal/mole}/0.6 = 2.4\,k_BT$, agrees nearly perfectly with the theoretical estimate (33) for the entropy loss of an end grafted chain of length $N = 156$, $\Delta S = k_B \ln\sqrt{N} \simeq 2.5\,k_B$.

Experiment versus simulation

From Table 1, it is apparent that for the nonphosphorylated protein on the PC/PS/PIP_2 and PC/PIP_2 membranes $\Delta F_{tail+loop}(\sim 2\,\text{kcal/mole})$ is considerably smaller than ΔF_{ED}, the binding free energy of MARCKS-ED, which implies that $\Delta F_{ED} \approx \Delta F$. In other words, for these protein-membrane systems, the binding free energy of the intact MARCKS and the MARCKS-ED peptide are of similar magnitudes, within $1 - 2\,\text{kcal/mole}$ of each other. This finding agrees reasonably well with experimental measurements of K_a, the partition coefficients of the peptide and protein between solution and a PC:PS = 90:10 membrane. Specifically, it was found that $K_a \approx 6 \times 10^3 M^{-1}$ for MARCKS-ED (41), and $K_a \approx 10^4\,M^{-1}$ for the intact MARCKS (42), implying $\Delta F(\text{MARCKS}) - \Delta F(\text{MARCKS-ED}) \approx -0.3\,\text{kcal/mole}$.

Partition coefficients of MARCKS and MARCKS-ED were also measured (using different methods (41,42)) for several other PC:PS membrane compositions. One intriguing finding is that upon increasing [PS] from 10% to 20%, the binding constant of MARCKS-ED increases ~1000-fold (reflecting the stronger attraction of its basic residues to the membrane), whereas the corresponding increase in MARCKS binding is only ~10-fold. The more moderate enhancement of MARCKS binding may be attributed to the concomitant increase in the electrostatic repulsion of the tail and loop chains from the membrane (S. McLaughlin, Stony Brook University, personal communication, 2007). We have not carried out systematic simulations of PC/PS membranes and thus cannot test this behavior quantitatively.

Our calculations may be compared to binding measurements of MARCKS and MARCKS-ED to electrically neutral membranes, which yielded $K_a = 2.6 \times 10^3\,M^{-1}$ (or $\Delta F = -4.7\,\text{kcal/mole}$) (42) and $K_a \approx 50\,M^{-1}$ ($\Delta F \approx -2.3\,\text{kcal/mole}$) (41), respectively. The difference, $\Delta(\Delta F) = -4.7 - (-2.3) = -2.4\,\text{kcal/mole}$, may be interpreted as the binding free energy of the tail and loop domains to the neutral membrane. Our simulations of the electrically neutral tail and loop (whose interactions with charged and neutral membranes are no different) yield a comparable value: $\Delta F_{tail+loop} = -3.4\,\text{kcal/mole}$.

In Table 1, we also report our estimates, based on Eq. 17, for the molar partition coefficients, $K_a = [LP]/[L][P]$, of the MARCKS-ED peptide, its FA mutant, and their phosphorylated isomers. (In all cases $a_L = 65\,\text{Å}^2$, with λ in the range $5\,d$–$15\,d$, depending on the system modeled, so that $K_a^{ED}([M]^{-1}) = 3.39(\lambda/10\,d) \times \exp(-\Delta F_{ED}(\text{kcal/mole})/0.6)$.) These values may be compared to experimental results obtained for similar systems, as shown for several cases in Table 2.

TABLE 2 Measured and calculated binding constants, in M^{-1}. M and M-ED stand for MARCKS and MARCKS-ED, respectively

PC:PS:PIP_2 & protein (Experiment reference)	100:0:0 & M-ED (41,44)	100:0:0 & M (42)	93:6:1 & M-ED (9)	89:10:1 & M-ED	90:10:0 & M-ED (41,44)	90:10:0 & M (42)	99:0:1 & M-ED (44)
K_a (experiment)	50	2.6×10^3	5×10^5		6×10^3	1.1×10^4	1×10^6
K_a (simulation)	(See text)			2×10^6	4×10^2	6×10^3	2×10^4

PC:PS:PIP_2 = 89:10:1, etc., denote the membrane composition.

Electrostatic-hydrophobic coupling

We close this section with a few comments on the insertion energies of the hydrophobic ED residues, aiming to highlight certain aspects of their coupling to electrostatic effects. The difference in adsorption free energy upon replacing a phenylalanine group of a short, uncharged peptide by alanine was determined experimentally as 1.3 kcal/mole (36) (see Appendix A). On the other hand, the ratio between the partitioning of MARCKS-ED and MARCKS-FA-ED to PC/PS = 10:1 membranes was found to range between 6 and 10, implying a difference of 0.22–0.27 kcal/mole in the binding free energy per residue (43,44). For a different membrane, PC/PIP_2 = 99:1, this ratio was found to be 300, corresponding to a free energy difference of 0.7 kcal/mole per residue (45). From our calculations, as given in Table 1, we conclude that the difference in the binding energy per residue, $\Delta(\Delta F) = (\Delta F_{\text{MARCKS-ED}} - \Delta F_{\text{MARCKS-FA-ED}})/5$, ranges between 0.36 and 0.74 kcal/mole, comparable to the experimental results. The difference between the measurements involving the short hydrophobic peptides and those for MARCKS-ED may be attributed to the different ''environments'' surrounding the phenylalanine residues in the two types of peptides, as well as to their different sizes. This explanation is supported by the fact that our calculated values of $\Delta(\Delta F)$ above, which agree with the measured values for the MARCKS peptides (43,44), were derived using hydrophobic insertion potentials based on measurements involving the short hydrophobic peptides (36), (Appendix A). Qualitatively, the apparent discrepancy above between the two experimental values of $\Delta(\Delta F)$ can be explained as being due to the presence of charged amino acids (which tend to avoid the hydrophobic core) around the phenyl groups. The charged groups are ''repelled'' from the membrane surface due to their unfavorable Born energy, thus diminishing the ability of the phenyl groups to insert into the hydrophobic core. On the other hand, the inserted phenyl groups pull the charged amino acids of MARCKS-ED toward the membrane and hence to oppositely charged lipids, resulting in a larger contribution to the adsorption free energy as compared to MARCKS-FA-ED (shown in Table 1).

Adsorption isotherms—''electrostatic-switching''

Experiments reveal that under typical physiological conditions (bulk concentration of $\sim 1\ \mu$M), MARCKS-ED efficiently inhibits PIP_2 hydrolysis by phospholipase C (10,45), indicating that all PIP_2 lipids are bound. After phosphorylation, whereby the net charge on the ED drops from +13 to +7, the peptide desorbs, exposing the PIP_2 molecules to enzymatic reactions. Our goal in this section is to examine this behavior based on the ΔF values reported in Table 1. To this end, we use the Langmuir adsorption isotherm, Eq. 13, but with a minor redefinition of θ. Namely, because we are primarily interested here in PIP_2-containing membranes, we now use θ to denote the fraction of protein-bound PIP_2 molecules. More precisely, θ is calculated as the ratio $n_{PIP_2}([\bar{P}]/([\overline{PIP}_2])$, where $[\bar{P}]$ and $[\overline{PIP}_2]$ are the surface concentrations of membrane bound proteins and PIP_2 lipids, respectively. Interpreting n_{PIP_2} as the number of PIP_2 lipids sequestered and bound by one membrane adsorbed protein (or peptide), then $\theta = 1$ means that all such lipids are protein bound (possibly shielded from enzymatic attack). In the calculations reported below, we have used $n_{PIP_2} = 3$. More details on the calculation are given in Appendix B.

To calculate θ as a function of the equilibrium volume fraction (bulk concentration) of proteins, φ, we rewrite Eq. 13 in the form

$$\theta = \frac{\varphi e^{-\Delta F}}{1 + \varphi e^{-\Delta F}} \tag{19}$$

and calculate the adsorption isotherms using the binding free energies from Table 1. (The relationship between the volume fraction and the molar concentration is given in Appendix B). Adsorption isotherms for representative cases involving MARCKS, MARCKS-FA, MARCKS-ED, MARCKS-FA-ED, and their phosphorylated isomers are shown in Fig. 7. In addition to the two PIP_2-containing membranes, adsorption isotherms are also shown for the PC:PS = 90:10 membrane, in which case θ in Eq. 19 is simply the fraction of membrane area covered by adsorbed proteins.

For all membranes considered in Fig. 7, the intact proteins adsorb more strongly than the corresponding ED peptides, owing to their larger binding energies. We also note, as expected, that phosphorylation greatly weakens the binding. Similar behavior is predicted upon replacing the phenylalanines by alanines. For bulk protein concentrations of, say, $\varphi \sim 1\mu$M, our calculations suggest that θ is nonzero only for the PIP_2-containing membranes. Specifically, for this bulk concentration of MARCKS in equilibrium with a PC/PS/PIP_2 = 89:10:1 membrane, we find that $\theta = 1$, i.e., the ratio between membrane-bound proteins to PIP_2 lipids is $\sim$1:3. If a membrane-bound protein indeed sequesters and binds $\sim$3

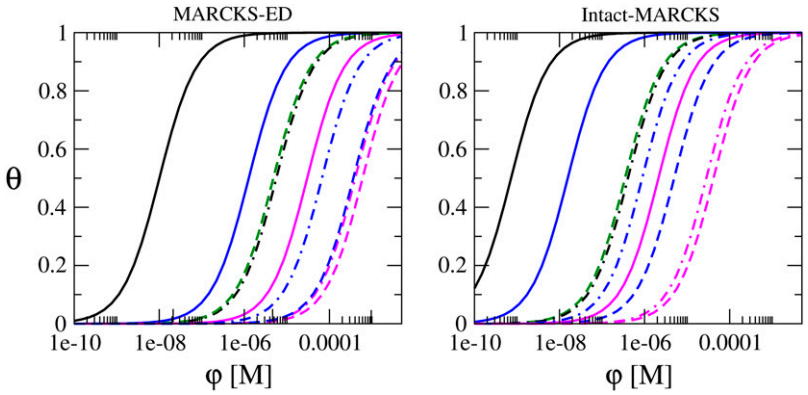

FIGURE 7 Adsorption isotherms for the MARCKS-ED peptide (*left*) and intact-MARCKS protein (*right*). The fraction of occupied adsorption membrane sites (which equals the fraction of bound PIP_2s in membranes containing these lipids) is plotted here as a function of the MARCKS concentration in solution, for PC:PS:PIP_2 = 89:10:1 (*black* or *green*), PC:PIP_2 = 99:1 (*blue*), and PC:PS = 90:10 (*purple*) membranes. The solid, dashed, and dash-dotted curves correspond to MARCKS (peptide and protein), MARCKS-FA, and the phosphorylated MARCKS, respectively.

PIP_2s, it is reasonable to assume that it will shield them from hydrolyzing enzymes. After phosphorylation θ drops sharply, implying partial exposure of these lipids to enzymatic attack, as suggested by the ''electrostatic-switch'' mechanism.

For bulk protein concentrations of, say, $\varphi \sim 10\,\mu$M (as found in some brain tissue cells, see Gambhir et al. (10) and references therein) we find that MARCKS adsorbs efficiently on the PC:PS = 90:10 membrane as well.

We are not aware of experimental results pertaining exactly to the systems we studied, yet comparing our results to those derived for two somewhat different systems reveals similar trends. More than 90% inhibition of PIP_2 hydrolysis in a PC:PS:PIP_2 = 66:33:1 membrane has been observed for 0.1 μM MARCKS-ED in solution, and ~50% inhibition with 0.3–0.5 μM MARCKS-ED for a PC:PS:PIP_2 = 83:17:0.15 membrane (10,45). For bulk protein concentrations in this regime (0.1–1 μM), our simulations of MARCKS-ED indicate $\theta \sim 1$ for the PC:PS:PIP_2 = 89:10:1 membrane, and $\theta \sim 0.2 - 0.5$ for the PC:PIP_2 = 99:1 membrane (Fig. 7).

Many experimental studies so far have focused on the role of PIP_2 in the binding of basic proteins and peptides to acidic membranes (5,6,17). One, still somewhat controversial issue, is whether polybasic peptides are adsorbed via nonspecific electrostatic attraction to the oppositely charged membrane, or specifically need polyvalent lipids to mediate their binding, (see Discussion in McLaughlin (5)). Our calculations cannot resolve this issue, yet they suggest that the bound proteins indeed sequester PIP_2 molecules, which significantly enhances their binding as compared to membranes devoid of these multivalent lipids.

CONCLUDING REMARKS

Using a detailed, albeit coarse-grained, ''molecular-level'' model to describe the configurations of the flexible MARCKS protein, we have carried out several series of Monte Carlo simulations, mimicking MARCKS binding to mixed, fluid, lipid membranes. Particular emphasis was devoted to the role of lipid lateral mobility and the ability of the adsorbed proteins to sequester and bind the multivalent acidic PIP_2 lipids. We found that MARCKS adsorbs effectively on membranes containing ~1% of these lipids, attracting them to their vicinity. Upon phosphorylation, which halves the net charge on the basic domain, the binding is weakened substantially. Depending on the protein concentration in the cell, the phosphorylation may induce a sharp transition from a state where the PIP_2s are shielded by the adsorbed protein to a state where they are exposed to enzymatic attack, thereby initiating their role as second messengers in signal transduction events.

On a more general level, the simulations demonstrate the subtle interplay between the various entropic and energetic contributions to the binding free energy of MARCKS and other flexible proteins. For instance, we found that the sum of configurational entropy losses experienced by the flexible loop and tail chains counterbalance most of the binding energy gained due to the myristoyl anchor. Our simulations have also revealed an interesting correlation between the hydrophobic attraction of the effector domain due to the phenylalanine side chains and the electrostatic attraction of the basic residues to acidic lipids.

Many of the ''quantitative'' conclusions derived from our simulations depend sensitively on estimates of such quantities like the hydrophobic membrane insertion energies of the myristoyl anchor or the phenylalanines, the use of DH electrostatic potentials, or the depiction of the protein as a freely jointed chain of spherical beads. Any error in estimating these quantities may affect the numbers obtained. Furthermore, although we allow for lateral lipid mobility, our simulations do not explicitly account for kinetic timescales, such as the diffusion times of different lipid species, or the rates of protein adsorption-desorption, whose relative magnitudes can play a major role in determining the extent of acidic lipid binding and protein-membrane interaction (46). Notwithstanding these reservations, we reiterate that our main goal here has been to explore and highlight some of the most general qualitative mechanisms underlying the adsorption of charged and unstructured proteins on oppositely charged-mixed-fluid membranes. Our approximate model has unambiguously revealed the crucial role played by lipid mobility

and polyvalent lipid sequestration in protein-membrane interaction, and demonstrated the delicate balance between the electrostatic, hydrophobic, and entropic components of this interaction.

APPENDIX A

Our parameterization of the well depths D_h appearing in the hydrophobic interaction potentials defined in Eq. 7 is based on two series of experiments performed by Wimley and White (36). In one series of experiments (Experiment I), partition coefficients (or, equivalently, transfer free energies ΔG^0) were measured for a series of peptides of different lengths: acetyl-WL, acetyl-WLL,. . ., acetyl-WL_6 (W, tryptophan, L, leucine), finding that ΔG^0 increases linearly with peptide length, with a slope of 0.56 kcal/mole, which was interpreted as the free energy of transferring leucine from membrane to water. The second set of experiments (Experiment II) involved pentapeptides of the form acetyl-WLXLL, where X is one of the 20 natural amino acids. The transfer free energies for the amino acids of interest here are: 1), For X = A = alanine, $\Delta G_{WLALL} = 4.08 \pm 0.03$ kcal/mole; 2), For X = F = phenylalanine, $\Delta G_{WLFLL} = 5.38 \pm 0.02$ kcal/mole; 3), For X = L = leucine, $\Delta G_{WLLLL} = 4.81 \pm 0.02$ kcal/mole; 4), For X = W = tryptophan, $\Delta G_{WLWLL} = 6.10 \pm 0.02$ kcal/mole.

Using our simulation to mimic Experiment I, we found that $D_{h,leu} = 2.4\,k_BT = 1.44$ kcal/mole reproduces the slope $\Delta(\Delta G^0(WL_n)) = 0.56$ kcal/mole mentioned above. Using this $D_{h,leu}$ in simulating Experiment II-3, we found $D_{h,trp} = 4.7\,k_BT = 2.82$ kcal/mole. Then, using these two values to simulate Experiments II-1 and II-2, we determined $D_{h,ala}$ and $D_{h,phe}$, respectively. Although not needed for our MARCKS simulations (since W does not appear in MARCKS-ED), we have carried out a ''control simulation'' corresponding to Experiment II-4, finding that our previously determined $D_{h,leu}$ and $D_{h,trp}$ indeed reproduce the experimental ΔG_{WLWLL}. Based on the procedure outline above, we found: $D_{h,leu} = 2.4\,k_BT = 1.44$ kcal/mole, $D_{h,ala} = 0.7\,k_BT = 0.42$ kcal/mole, and $D_{h,phe} = 3.5\,k_BT = 2.1$ kcal/mole.

APPENDIX B

Recall that on PIP_2-containing membranes, each adsorbed protein sequesters $n_{PIP_2} \approx 3 - 4$ PIP_2 lipids (hereafter, for concreteness, we assume $n_{PIP_2} = 3$), which on the bare membrane spread over an (average) area $\tilde{a}$, possibly larger than the projected area of an adsorbed protein. (For example, in a membrane containing 1% PIP_2, the average area enclosing three PIP_2s is $\tilde{a} \approx 300\,d^2$, whereas the area ''shaded'' by one adsorbed MARCKS-ED is $a \approx 100\,d^2$ (see Fig. 4). For the intact MARCKS, our calculations yield $a \simeq \tilde{a} \approx 300\,d^2$.) In the lattice model formulation leading to Eq. 13, the definition of θ as the fraction of bound PIP_2s simply means that the membrane is an array of adsorption cells of area $\tilde{a}$, accommodating no more than one adsorbed protein.

If $a < \tilde{a}$, then when all PIP_2s are bound ($\theta = 1$), there is an ''excess membrane area'' ($\tilde{a} - a$ per adsorbed peptide), which, in principle, may accommodate additional proteins. Yet, adsorption onto these PIP_2 deficient regions—which is mediated by the insertion of hydrophobic side chains into the bilayer's core, and/or by electrostatic attraction to the monovalent PS lipids—is relatively weak, and therefore not included in our calculation of θ for the two PIP_2 containing membranes. The minor contribution to adsorption from these regions can be estimated based on adsorption isotherms for the PC:PS = 90:10 membrane; as shown below. (Of course, for membranes containing higher concentrations of PS, this contribution can be significant.) Choosing the area per molecule equal to $\tilde{a}$ (as defined above) enables direct comparison between membranes containing PIP_2 with those depleted of this lipid.

For comparison with experiment, recall that $\varphi \equiv \nu N_P/V = \nu[P]$ in Eq. 13 is the volume fraction of proteins in solution, which is proportional to their molar concentration $[P]/N_0$; N_0 is Avogadro's number and $\nu = \lambda a \cong 10 \times 8.66 \times \pi(5.5 \times 8.66)^2$ Å^3, corresponding to a molar volume of 400 M^{-1}; so that for a typical bulk concentration of proteins (around 1 μM), $\varphi \approx 4 \times 10^{-3}$ (We have again used here $r_{max} = 5.5\,d = 5.5 \times 8.66$ Å; $\lambda \approx 10\,d$ is the calculated thickness of the adsorption layer.)

We are grateful to Stuart McLaughlin for his critical, constructive, and encouraging comments. We also thank Vladimir Teif and Daniel Harries for helpful discussions.

We thank the US-Israel Binational Science Foundation (BSF grants 2002-75 and 2006-401, D.M. and A.B.S.) and the Israel Science Foundation (ISF grant 659/06, A.B.S.) for financial support. The Fritz Haber research center, where all calculations were carried out, is supported by the Minerva foundation, Germany.

REFERENCES

1. Hosaka, M., R. E. Hammer, and T. C. Sudhof. 1999. A phospho-switch controls the dynamic association of synapsins with synaptic vesicles. *Neuron*. 24:377–387.
2. Ono, A., S. D. Ablan, S. J. Lockett, K. Nagashima, and E. O. Freed. 2004. Phosphatidylinositol (4,5) bisphosphate regulates HIV-1 gag targeting to the plasma membrane. *Proc. Natl. Acad. Sci. USA*. 101: 14889–14894.
3. McLaughlin, S., and A. Aderem. 1995. The myristoyl-electrostatic switch: a modulator of reversible protein-membrane interactions. *Trends Biochem. Sci*. 20:272–276.
4. Murray, D., L. Hermida-Matsumoto, C. A. Buser, J. Tsang, C. T. Sigal, N. Ben-Tal, B. Honig, M. D. Resh, and S. McLaughlin. 1998. Electrostatics and the membrane association of Src: Theory and experiment. *Biochemistry*. 37:2145–2159.
5. McLaughlin, S. 2006. Tools to tamper with phosphoinositides. *Science*. 314:1402–1403.
6. Heo, W. D., T. Inoue, W. S. Park, M. L. Kim, B. O. Park, T. J. Wandless, and T. Meyer. 2006. PI(3,4,5)P-3 and PI(4,5)P-2 lipids target proteins with polybasic clusters to the plasma membrane. *Science*. 314:1458–1461.
7. Yeung, T., G. E. Gilbert, J. Shi, J. Silvius, A. Kapus, and S. Grinstein. 2008. Membrane phosphatidylserine regulates surface charge and protein localization. *Science*. 319:210–213.
8. Lodish, H., A. Berk, P. Matsudaira, C. A. Kaiser, M. Krieger, M. P. Scott, S. L. Zipursky, and J. Darnell. 2004. Molecular Cell Biology, 5th ed. Freeman, New York.
9. Wang, J., A. Arbuzova, G. Hangyás-Mihályné, and S. McLaughlin. 2001. The effector domain of myristoylated alanine-rich C kinase substrate binds strongly to phosphatidylinositol 4,5-bisphosphate. *J. Biol. Chem*. 276:5012–5019.
10. Gambhir, A., G. Hangyás-Mihályné, I. Zaitseva, D. S. Cafiso, J. Y. Wang, D. Murray, S. N. Pentyala, S. O. Smith, and S. McLaughlin. 2004. Electrostatic sequestration of PIP_2 on phospholipid membranes by basic/aromatic regions of proteins. *Biophys. J*. 86:2188–2207.
11. Laux, T., K. Fukami, M. Thelen, T. Golub, D. Frey, and P. Caroni. 2000. GAP43, MARCKS, and CAP23 modulate $PI(4,5)P_2$ at plasmalemmal rafts, and regulate cell cortex actin dynamics through common mechanism. *J. Cell Biol*. 149:1455–1471.
12. McLaughlin, S., J. Wang, A. Gambhir, and D. Murray. 2002. PIP_2 and proteins: Interactions, organization and information flow. *Annu. Rev. Biophys. Biomol. Struct*. 31:151–175.
13. Nelson, D. L., and M. M. Cox. 2004. Lehninger Principles of Biochemistry, 3rd ed. Worth, New York.
14. Revenu, C., R. Athman, S. Robine, and D. Louvard. 2004. The coworkers of actin filaments: from cell structures to signals. *Nat. Rev. Mol. Cell Biol*. 5:1–12.
15. Arbuzova, A., A. A. P. Schmitz, and G. Vergeres. 2002. Cross-talk unfolded: MARCKS proteins. Part 1. *Biochem. J*. 362:1–12.

16. Myat, M. M., S. Anderson, L. H. Allen, and A. Aderem. 1997. MARCKS regulates membrane ruffling and cell spreading. *Curr. Biol.* 7:611–614.

17. Murray, D., and B. Honig. 2005. To B or not to B: PIP_2 answers the question. *Dev. Cell.* 8:138–139.

18. Murray, D., A. Arbuzova, B. Honig, and S. McLaughlin. 2002. The role of electrostatic and nonpolar interactions in the association of peripheral proteins with membranes. *Curr. Top. Membr.* 52:277–307.

19. Tzlil, S., and A. Ben-Shaul. 2005. Flexible charged macromolecules on mixed fluid lipid membranes: theory and Monte Carlo simulations. *Biophys. J.* 89:2972–2987.

20. Rosenbluth, M. N., and A. W. Rosenbluth. 1955. Monte Carlo simulations of the average extension of molecular chains. *J. Chem. Phys.* 23:356–359.

21. Frenkel, D., and B. Smit. 1996. Understanding Molecular Simulation: From Algorithms to Applications. Academic Press, New York.

22. Harries, D., S. May, W. M. Gelbart, and A. Ben-Shaul. 1998. Structure, stability and thermodynamics of lamellar DNA-lipid complexes. *Biophys. J.* 75:159–173.

23. May, S., D. Harries, and A. Ben-Shaul. 2000. Lipid demixing and protein-protein interactions in the adsorption of charged proteins on mixed membranes. *Biophys. J.* 79:1747–1760.

24. Murray, D., A. Arbuzova, G. Hangys-Mihalyne, A. Gambhir, N. Ben-Tal, B. Honig, and S. McLaughlin. 1999. Electrostatic properties of membranes containing acidic lipids and adsorbed basic peptides: theory and experiment. *Biophys. J.* 77:3176–3188.

25. Wang, J. Y., A. Gambhir, S. McLaughlin, and D. Murray. 2004. A computational model for the electrostatic sequestration of $PI(4,5)P_2$ by membrane-adsorbed basic peptides. *Biophys. J.* 86: 1969–1986.

26. May, S., D. Harries, and A. Ben-Shaul. 2002. Macroion-induced instability of binary fluid membranes. *Phys. Rev. Lett.* 89:268102.

27. Mbamala, E. C., A. Ben-Shaul, and S. May. 2005. Domain formation induced by the adsorption of charged proteins on mixed lipid membranes. *Biophys. J.* 88:1702–1714.

28. Teif, V. B., D. Harries, D. Lando, and A. Ben-Shaul. 2008. Matrix formalism for site-specific binding of unstructured proteins to multicomponent lipid membranes. *J. Pept. Sci.* 14:368–373.

29. Skolnick, J., and M. Fixman. 1977. Electrostatic persistence length of a wormlike polyelectrolyte. *Macromolecules.* 10:944–948.

30. Odijk, T. 1977. Polyelectrolytes near rod limit. *J. Pol. Sci. B Pol. Phys.* 15:477–483.

31. Ellena, J. F., M. C. Burnitz, and D. S. Cafiso. 2003. Location of the myristoylated alanine-rich C-kinase substrate (MARCKS) effector domain in negatively charged phospholipid bicelles. *Biophys. J.* 85: 2442–2448.

32. MARCKS_HUMAN. 2007. Swiss-Prot. http://www.expasy.org/uniprot/P29966.

33. Fleer, G., M. C. Stuart, J. M. H. M. Scheutjens, T. Cosgrove, and B. Vincent. 1998. Polymers at Interfaces. Chapman & Hall, New York.

34. Gerroff, I., A. Milchev, K. Binder, and W. Paul. 1993. A new off-lattice Monte-Carlo model for polymers - a comparison of static and dynamic properties with the bond-fluctuation model and application to random-media. *J. Chem. Phys.* 98:6526–6539.

35. Netz, R. R. 1999. Debye-Huckel theory for interfacial geometries. *Phys. Rev. E Stat.* 60:3174–3182.

36. Wimley, W. C., and S. H. White. 1996. Experimentally determined hydrophobicity scale for proteins at membrane interfaces. *Nat. Struct. Biol.* 3:842–848.

37. Haleva, E., N. Ben-Tal, and H. Diamant. 2004. Increased concentration of polyvalent phospholipids in the adsorption domain of a charged protein. *Biophys. J.* 86:2165–2178.

38. Khelashvili, G., H. Weinstein, and D. Harries. 2008. Protein diffusion on charged membranes: a dynamic mean-field model describes time evolution and lipid reorganization. *Biophys. J.* 94:2580–2597.

39. Rauch, M. E., C. G. Ferguson, G. D. Prestwich, and D. S. Cafiso. 2002. Myristoylated alanine-rich C kinase substrate (MARCKS) sequesters spin-labeled phosphatidylinositol 4,5-bisphosphate in lipid bilayers. *J. Biol. Chem.* 277:14068–14076.

40. Tapp, H., I. M. Al-Naggar, E. G. Yarmola, A. Harrison, G. Shaw, A. S. Edison, and M. R. Bubb. 2005. MARCKS is a natively unfolded protein with an inaccessible actin-binding site. *J. Biol. Chem.* 280:9946–9956.

41. Rusu, L., A. Gambhir, S. McLaughlin, and J. Rädler. 2004. Fluorescence correlation spectroscopy studies of peptide and protein binding to phospholipid vesicles. *Biophys. J.* 87:1044–1053.

42. Kim, J. Y., T. Shishido, X. L. Jiang, A. Aderem, and S. McLaughlin. 1994. Phosphorylation, high ionic-strength, and calmodulin reverse the binding of MARCKS to phospholipid vesicles. *J. Biol. Chem.* 269: 28214–28219.

43. Victor, K., J. Jacob, and D. S. Cafiso. 1999. Interactions controlling the membrane binding of basic protein domains: Phenylalanine and the attachment of the myristoylated alanine-rich C-kinase substrate protein to interfaces. *Biochemistry.* 38:12527–12536.

44. Arbuzova, A., L. Wang, J. Wang, G. Hangyás-Mihályné, D. Murray, D. Honig, and S. McLaughlin. 2000. Membrane binding of peptides containing both basic and aromatic residues. Experimental studies with peptides corresponding to the scaffolding region of caveolin and the effector region of MARCKS. *Biochemistry.* 39:10330–10339.

45. Wang, J. Y., A. Gambhir, G. Hangyás-Mihályné, D. Murray, U. Golebiewska, and S. McLaughlin. 2002. Lateral sequestration of phosphatidylinositol 4,5-bisphosphate by the basic effector domain of myristoylated alanine-rich C kinase substrate is due to nonspecific electrostatic interactions. *J. Biol. Chem.* 277:34401–34412.

46. Golebiewska, U., M. Nyako, W. Woturski, I. Zaitseva, and S. McLaughlin. 2008. Diffusion coefficient of fluorescent phosphatidylinositol 4,5-bisphosphate in the plasma membrane of cells. *Mol. Biol. Cell.* 19:1663–1669.